

UNCLASSIFIED

AD 297 065

*Reproduced
by the*

ARMED SERVICES TECHNICAL INFORMATION AGENCY
ARLINGTON HALL STATION
ARLINGTON 12, VIRGINIA



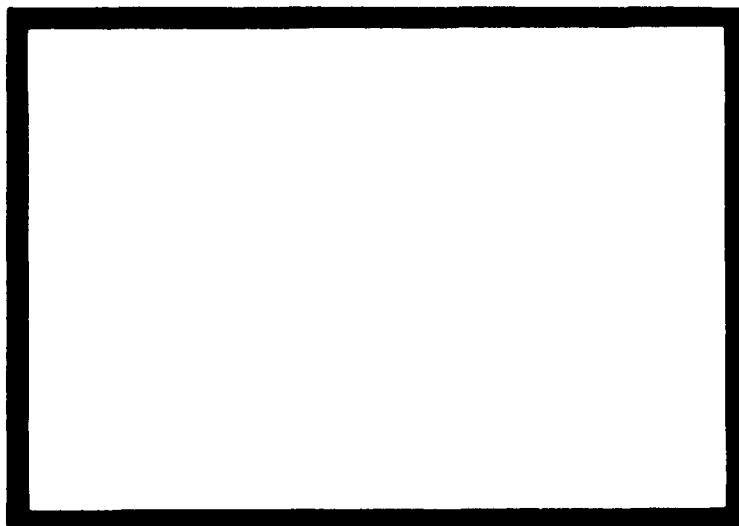
UNCLASSIFIED

NOTICE: When government or other drawings, specifications or other data are used for any purpose other than in connection with a definitely related government procurement operation, the U. S. Government thereby incurs no responsibility, nor any obligation whatsoever; and the fact that the Government may have formulated, furnished, or in any way supplied the said drawings, specifications, or other data is not to be regarded by implication or otherwise as in any manner licensing the holder or any other person or corporation, or conveying any rights or permission to manufacture, use or sell any patented invention that may in any way be related thereto.

297 065

CATALOGED BY ASTIA
AS AD 29 2065
MECHANICAL
HNOLOGY
INCORPORATED

ASTIA
RECEIVED
FEB 27 1963
RESOLVED
TISIA A



MTI-62TR40

**EXPERIMENTAL INVESTIGATION OF
TWO-PHASE FLOW IN THRUST BEARINGS**

by

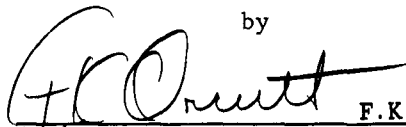
F. K. Orcutt

**Contract Nonr-3731(00)(FEM)
Task No. NR319-438**


January 1963

EXPERIMENTAL INVESTIGATION OF
TWO-PHASE FLOW IN THRUST BEARINGS

by


F.K. Orcutt
Author


C.H.T. Pan
Approved by


B. Sternlicht
Approved by

Prepared under

Contract No. Nonr-3731(00)(FBM)

Task No. NR391-438

Administered by

OFFICE OF NAVAL RESEARCH

Department of the Navy

Reproduction in Whole or in Part is Permitted
for any Purpose of the U. S. Government

MECHANICAL TECHNOLOGY INCORPORATED

LATHAM, NEW YORK

TABLE OF CONTENTS

| | Page |
|--|------|
| 1.0 INTRODUCTION | 1 |
| 2.0 PHYSICAL PRINCIPLE OF VAPOR LUBRICATION..... | 2 |
| 3.0 STEAM-LUBRICATED THRUST BEARING APPARATUS..... | 4 |
| 4.0 EXPERIMENTAL STEAM-LUBRICATED BEARING OPERATION..... | 7 |
| 4.1 Bearing Stiffness and Load Carry Capacity..... | 9 |
| 4.2 Film Pressure Distribution..... | 12 |
| 4.3 Stationary Surface Temperature..... | 15 |
| 4.4 Steam-Coolant Heat Balance..... | 17 |
| 4.5 Effect of Superheat..... | 18 |
| 4.6 Erosion of the Bearing Elements..... | 18 |
| 5.0 CONCLUSIONS..... | 19 |
| 6.0 RECOMMENDATIONS..... | 20 |
| 7.0 LIST OF REFERENCES..... | 21 |

1.0 INTRODUCTION

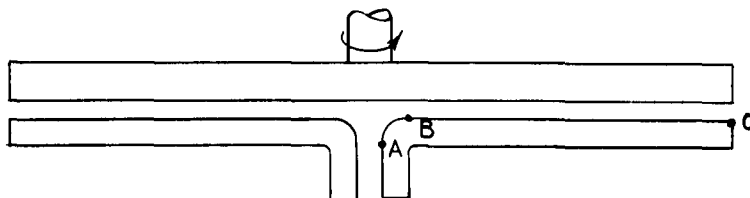
There are numerous rotating machinery applications wherein the use of the process fluid as the bearing lubricant in place of more conventional lubricants is extremely advantageous or even essential. The trend toward this lubrication concept is illustrated by the extensive recent research aimed at developing practical high-performance machinery operating on bearings lubricated by gases and such non-lubricating liquids, in the conventional sense, as liquid metals and water. Another class of process fluids which might be used as lubricants are those which are vapors at the working temperature and pressure, such as steam.

The behavior of vapors in bearings should be quite different from that of gases. Thermodynamic processes are treated simply in gas-lubricated bearings while they are likely to both be more complex and more important in vapor-lubricated bearings. Under most practical operating conditions, condensation can be expected to occur in vapor-lubricated bearings. Consequently, the vapor-lubricated bearing problem is one of two-phase flow. An analytical study of two-phase flow in thrust bearings is being conducted.

(1) This report describes the results of the concurrent experimental investigation. Thus far, the experiments have been largely exploratory and, as such, were intended to provide a better appreciation of the nature of the phenomena occurring in vapor-lubricated bearings and of the broad practical significance of these phenomena.

2.0 PHYSICAL PRINCIPLES OF VAPOR LUBRICATION

In its simplest form externally pressurized bearing consists of two flat surfaces separated by the lubricant, which is supplied from a center-located inlet as shown in the sketch below.



This is essentially the configuration for this investigation. In an actual application, either or both of the bearing elements might be maintained at a temperature below that of the entering lubricant. If a condensable lubricant is used, phase change from vapor to liquid can take place near this cooled surface. To study the significance of condensation in such a vapor bearing, an experiment is carried out with the stationary lower plate cooled in a controlled fashion. The upper rotating plate is not cooled and is made of a low conductivity material in order to present, as nearly as possible, an adiabatic upper boundary for the lubricant film. The reverse situation, in which the rotating plate is cooled instead of the stationary plate, is also of interest and it is planned to investigate this arrangement later.

Some conception of the flow processes within the bearing may be had from consideration of the physical system and inspection of the Mollier Chart for steam. The lubricant flow path in the bearing may be divided into two sections; A-B which is called the nozzle area, and B-C which will be referred to as the bearing area. Within the nozzle area, the bulk of the vapor expands by a flow process which is approximately isentropic and which is represented by the path ab on the Mollier Chart (Figure 1). This expansion is characterized by a reduction in vapor quality so that minute droplets of liquid are formed and entrained in the vapor. Some of the vapor adjacent to the cool walls of the nozzle will condense, forming a film

of liquid on these surfaces. A process of mass transfer from the vapor layer to the liquid film is represented by a series of isobaric paths such as a'd on the Mollier Chart. Since the cooled surface area in the nozzle is small, the rate at which surface condensation occurs is probably also small. Several influences will act on the liquid in the surface film tending to induce flow. These influences include the pressure gradient in the overlying vapor film and viscous drag forces at the vapor-liquid interface which will induce radially outward flow of the liquid. Circumferential drag forces will also be present if the opposing surface is rotating. In the nozzle area the pressure gradients are large so this effect probably dominates liquid film flow.

In the bearing area, the vapor will continue to expand and flow outward by a process which should resemble that described by the path from b to c on the Mollier Chart. Some further reduction in vapor quality and an increase in entrained liquid may occur during this process. Additional cooling and condensation of vapor close to the cooled surface will take place resulting in a progressive reduction in the mass flow rate of vapor with increasing distance from the inlet. This process is represented on the Mollier Chart by another series of isobaric (mass transfer) paths, as for example b'd and b''d''. Pressure gradient and drag forces will continue to act on the liquid film inducing outward flow. The drag forces should assume greater importance in the bearing area since pressure gradients are lower and surface separation are smaller than in the nozzle area.

Along the entire lubricant flow path in the bearing there exists a close linking or interdependence of the vapor and liquid flow processes. The pressure gradient and drag factors influencing liquid flow are obviously dependent on conditions in the overlying vapor layer. The thickness and surface contour of the liquid film in turn alter the geometry of the vapor flow path.

From the foregoing discussion it is apparent that the present understanding of vapor lubrication is quite superficial and is not firmly established. The experimental results which will be described were obtained in the initial phase of an experimental investigation aimed at further development of this understanding and verification of the results of a concurrent theoretical study.

3.0 STEAM-LUBRICATED THRUST BEARING APPARATUS

A flat plate, externally pressurized thrust bearing having one center-located bell mouthed inlet was chosen as the bearing configuration for the investigation because of its comparative simplicity and because it is the configuration used in the theoretical investigation. The main features of the bearing are shown in Figure 2. The 6 inch diameter rotor is a flat glass disk cemented to the end of the spindle. Glass was chosen for one of the bearing elements to permit visual observation of the bearing interface during operation. The aluminum stationary element has a helical coolant flow passage machined into it and pressure taps and thermocouples are mounted in it. The steam inlet at the center of the stator has a 0.312 inch diameter inlet tube and flares smoothly outward to blend into the flat surface at a diameter of 0.624 inches. When the surface separation is 10 mils, there is a 4 to 1 reduction in flow path area from the inlet tube to the annular region at the blending radius. This inlet design was chosen for simplicity and to avoid flow separation in the nozzle.

Stator surface temperature and film pressure are measured at each of six radii evenly spaced from $3/4$ inch to $2\ 3/4$ inch. Pressure measurements are made with 30 mil diameter taps, an 8 $1/2$ inch test-quality gage and the necessary arrangement of toggle valves to connect any one of the taps to the gage. Temperatures are measured to an estimated accuracy of $\pm 2^{\circ}\text{F}$ by sheathed copper-constantan thermocouples (40-mil sheath diameter) and a multipoint recorder. Pressure and temperature are measured in the throat of the steam inlet also.

The experimental bearing is mounted on, driven and loaded by a modified 15 inch drill press. Figure 3 is a photograph of the entire apparatus. Load is applied by weights suspended from the press feed lever. The press is equipped with a variable speed drive covering the range from 450 to 4700 rpm. The table of the press was modified to provide access for steam, instrumentation and coolant lines. Braces were added between the table and the head for stiffening and to permit some adjustment of the squareness of the stator surface to the spindle axis. With squareness obtained in this way, parallelism of the rotor

and stator surfaces is obtained by cementing the rotor to the spindle end with the rotor resting on the stator and light load applied.

Steam is supplied by a 18 KW electric steam generator rated at 100 psig maximum pressure, 60 lb/hour flow. This generator has proven to be adequate for most purposes however, at higher pressures especially, the range of operating conditions which could be investigated was restricted somewhat by its limited flow capacity. A 1.5 KW resistance wire heater is installed in the steam line to insure dry steam and if desired, to provide a limited amount of superheat. Steam quality can be measured by a throttling calorimeter installed in the line just ahead of the bearing inlet. Direct measurement of steam flow rate for the wide range of pressures and flow rates required is a difficult undertaking requiring multiple alternate sensing elements. For the sake of simplicity it was decided to make the measurement indirectly by measuring the feed water delivery rate necessary to maintain a constant water level in the generator. Admittedly this is an approximate measurement which has been complicated in practice by some fluctuation in feed water line pressure. A float-type flowmeter is used to measure feed water flow rate.

Separation of the surfaces was determined by measuring the location of the top surface of the rotor with a micrometer head mounted on the shroud surrounding the bearing. A hemispherical graphite tip is mounted on the end of the micrometer to permit measurements with the rotor turning. Reference measurements are made periodically by suddenly loading the bearing heavily to obtain zero separation with the apparatus at operating temperature. Measurements obtained with this simple arrangement have proven to be surprisingly reproducible and have an estimated accuracy of 0.0005 inch.

To conform to the situation investigated in the theoretical work as nearly as possible, the temperature distribution of the upper bearing surface should closely approach that of the steam in the gap; that is, it should be an adiabatic surface. The lower bearing surface should be at a nearly constant temperature which can be varied but which should generally be lower than the steam temperature. This situation is of practical significance since the bulk temperature of most machines will be lower than the process vapor temperature. Controlled and variable cooling of the stator is accomplished in the apparatus by pumping cool-

ing water through a helical passage. The passage size and pumping capacity were selected to give relatively high flow rates (up to about 40 lb/min) and low temperature rise (typically 4 to 12^oF). Coolant temperature is measured at inlet and outlet by thermocouples. Cooling rate is normally controlled by varying the coolant inlet temperature but it is possible to vary flow rate also by throttling the circulating pump or by adding cold water from the lines to the pump output. The coolant is heated by the exhaust steam from the bearing and, if necessary, by an in-line electric heater. Coolant temperature is controlled by a combination of the electric heater and controlled addition of cold water to the pump suction line.

Some warping of the bearing surfaces can be expected because of axial temperature gradients. The form of the expected distortion is dishing of the elements to produce convex bearing surfaces and diverging flow path boundaries. An approximate analysis was performed to obtain an order of magnitude estimate of the deviation from flatness which might be expected. The analysis assumed 100^oF temperature differences across the 3/4 inch rotor and across the 1/4 inch thick aluminum section separating the stator surface from the top surfaces of the coolant passages. It was also assumed that the elements distort without external restraint or internal stress. The calculation for the rotor indicated a total deviation from flatness or less than 0.001 inch. The combination of high expansivity and a thin section results in quite large predicted distortion of the aluminum plate (about 0.012 inch deviation from flatness). However, the aluminum plate is clamped to the base plate at the center by the steam inlet pipe and at the outer radius by cap screws so the actual distortion should be considerably lower.

4.0 EXPERIMENTAL STEAM-LUBRICATED BEARING OPERATION

The principal independent operating variables for the steam-lubricated bearing are steam conditions at inlet, coolant temperature and flow rate, load and rotational speed. The measured dependent variables include surface separation, steam flow rate, coolant temperature rise through the bearing, and film pressure and stator surface temperature distributions.

The effects of each of the independent variables on bearing behavior were determined for at least a limited range of the other independent variables. The usual experimental procedure was to fix all of the independent variables except load which was increased in steps until the surface separation was reduced to zero. The independent variable being investigated was then changed with the others held constant and the stepwise loading procedure was repeated.

Considerable data were accumulated during the performance of the experiments. Representative samples of data are presented in the following sections to illustrate the points which are made concerning the nature of the phenomena occurring during bearing operation.

VISUAL OBSERVATIONS

The appearance of the lubricant film can be classified into several characteristic types. Combinations of operating conditions which produced comparatively large surface separation and low cooling rate resulted in a film appearance marked by the near absence of any distinguishable features. A thin continuous film of condensate probably could be present on the stator surface without being detected because of the relatively high reflectivity of the aluminum surface.

Following a change in operating conditions tending to reduce surface separation or increase the cooling rate, small droplets appear in the gap near the outer radius. This condition is shown in Figure 4. The irregular dark patches visible in various areas are stains on the aluminum surface. It was not possible to determine conclusively on which surface the droplets had formed. If they were on the stator surface, their presence would deny the existence of a continuous liquid film on that surface. Another frequently observed feature of operation under these conditions is narrow radial streaks which emerge

from the nozzle area and which usually end before reaching the outer radius. These streaks appear to be drops of condensate which move rapidly outward leaving a wetted trail on the rotor surface. The streak ends when the drop is dissipated by formation of the trail which then gradually disappears. Periodic measurements of steam quality at the inlet tube have consistently shown moisture content of less than 2 percent. Therefore, it seems probably that the condensate drops coming from the nozzle area are formed in the nozzle and are not entrained in the steam supply.

Additional reductions in surface separation or increases in cooling rate eventually bring about a marked change in film appearance. A band-like zone appears around the outer edge of the bearing in which there are numerous large droplets which move slowly outward leaving wetted trails. Around these fully wetted areas the surface has an opaque, cloudy appearance (Figure 5). The overall appearance of this area is very much like that seen on a vertical, cold glass surface exposed to warm, moist air. After close inspection of this area with a pocket magnifier on several occasions it was concluded that the drops are formed on the glass and not on the aluminum surface.

Further change in operating conditions in the same direction as before causes the inner boundary of the previously described band to move inward and a second outer boundary appears. Except for scattered bubbles, the film is transparent outside the outer boundary and it is clear that the gap is completely bridged by condensate at this boundary. (Figure 6). The bubbles are apparently air which was dissolved in the feed water and which became entrained in the steam.

Once the complete condensation boundary appears, a small additional change in operating conditions is usually sufficient to cause it to move rapidly inward and the surfaces come together and contact. The photographs of film appearance, Figures 4 through 7, were taken with the shaft stationary. Essentially the same phenomena were observed when the shaft was rotating but the details of film appearance are obscured in the photographs taken with rotation.

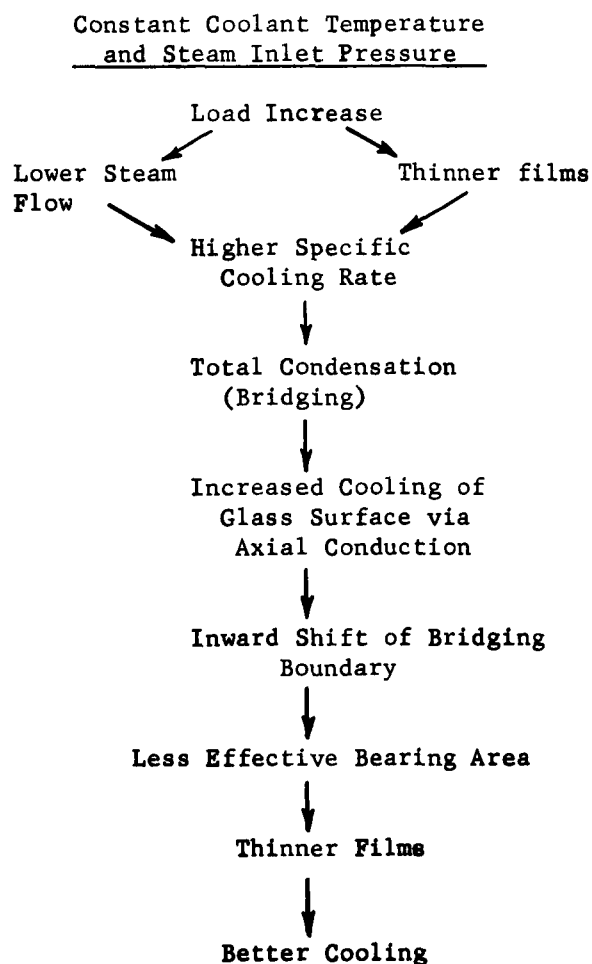
4.1 BEARING STIFFNESS AND LOAD CARRYING CAPACITY

Representative samples of the data showing change in surface separation with changing load are plotted in Figures 8 and 9. The striking feature of all of these data is the sudden loss of bearing stiffness at some critical load which results in sudden collapse of the bearing load carrying capacity. The sharp loss of stiffness follows quickly after the appearance of the bridging boundary which was just described. The rapid ensuing loss of surface separation is accompanied by an inward translation of the bridging boundary. As shown in Figure 8 bearing stiffness and the critical load for collapse of the bearing are strongly dependent on the rate of heat withdrawal from the film as controlled by coolant temperature. The extent of this dependence is illustrated by a comparison of the bearing stiffnesses just before collapse at various coolant temperatures for 60 psig inlet steam pressure. With 100 F coolant, bearing stiffness was about 11,000 lb/in. Raising coolant temperature to 170 F raised the stiffness to about 54,000 lb/in and when the coolant was drained from the system the stiffness was about 125,000 lb/in.

As expected, bearing stiffness and critical load were also dependent on steam inlet pressure as shown in Figure 9. Over the limited range investigated, the maximum load which could be supported was approximately proportional to the square of the inlet pressure. Part of this increase in load carrying capacity is the straightforward increase in film pressure with a given gap when the inlet pressure is raised. In addition to this, there is a significant reduction in the surface separation corresponding to the critical load when the inlet pressure is raised which further enhances the improvement in load carrying capacity. An increase in inlet pressure would be expected to reduce the surface separation at which bridging first occurs because of higher steam velocities in the gap and lower transit time of steam through the bearing so that the rate of condensation per pound of steam may be lower in spite of improved heat transfer and a high absolute rate of condensation. Another contributing factor is the increase in the specific enthalpy of saturated steam as the pressure is raised.

Bearing performance was essentially independent of rotational speed within the range of 450 to 2000 rpm. However, when the shaft was stationary, the critical load was usually slightly higher and the collapse less sudden (Figure 9). This observation can probably be attributed to higher breakaway friction of the drill press spindle when the shaft was not rotating.

The experimental evidence suggests that the characteristic sudden collapse of the steam lubricated bearing is caused by mutually reinforcing heat transfer, thermodynamic and lubrication effects. The sequence of events and their interactions which appear to explain this phenomenon are illustrated by the schematic diagram below:



The pressure in the liquid film outside the bridging boundary must be very close to the ambient so the bridging boundary effectively represents a reduced bearing radius. Therefore, once the bridging boundary is established, heat transfer and lubrication effects interact to initiate mutually reinforcing changes in surface separation and boundary radius.

On occasion a low frequency axial vibration or hammer was observed during bearing operation with the shaft stationary and a load close to the critical level. A large amplitude radial oscillation of the bridging boundary accompanies the vibration suggesting that the range of the vibratory displacement lies within the region of low stiffness accompanying collapse. Apparently the vibration is initiated by some transient effect which initiates collapse but the process is reversed by the increase in the film pressure caused by the decreasing surface separation. Cyclic fluctuation in load accompanying the initial surface movements then leads to the sustained vibration. The vibration is usually damped out within a few seconds.

4.2 FILM PRESSURE DISTRIBUTION

From theoretical considerations and previously described experimental results, both the shape of the pressure profile across the bearing and the absolute values of pressure can be expected to differ significantly for different cooling rates. This is the case as shown in Figures 10, 11 and 12. The absolute values of film pressure are considerably lower at higher cooling rates which is commensurate with the lower load carrying capacity. Increased cooling also shifts the effective radius of the distributed pressure inward. That is, the pressure gradients are steeper near the inlet and more gradual near the outer radius when the rate of heat loss from the film is increased. This is the expected effect of more rapid condensation of steam within the film and on the cooled surfaces.

Curves of theoretical film pressure distribution for a single-phase lubricant having the properties of dry steam are shown in Figures 10 through 12 for comparison with the experimental curves. The computations were based on the results given in Reference 2 using the same surface separation as was measured for the lowest load experimental case and a value of lubricant exit velocity calculated from the measured steam flow rate, the surface separation, and the assumption that saturated steam flows from the bearing exit. The effects of progressive condensation as the steam flows through the gap are apparent in the differences in shape of the experimental and theoretical curves which become greater as the coolant temperature was reduced.

The absolute values of calculated pressure for the single-phase lubricant are lower than would be expected for the same inlet pressure and allowance for the effects of condensation in the experimental bearing. That is, the theoretical curves should lie above the experimental curves at all points instead of crossing over below the experimental points near the inlet. Further, the film pressures, and thus the load capacity, of the theoretical single-phase lubricant bearing should become increasingly larger than the experimental values as the coolant temperature is reduced instead of becoming increasingly

lower as indicated in Figures 10 through 12. The explanation for the unexpected differences between experimental and theoretical curves is not entirely clear. However, it may be significant that the anticipated result is readily achieved if the surface separation used in calculating theoretical curves is reduced below the experimentally measured value. This is illustrated by the theoretical curve shown in Figure 12 for 6.5 mils surface separation instead of the 8.5 mils separation which was measured. A film of condensate on the cooled surface would reduce the effective gap width below the measured separation but it is highly unlikely that the condensate film could be sufficiently thick to account for so large a difference. Thermal distortion of the surfaces as discussed in the section on apparatus would reduce the surface separation at the inlet below the mean separation. When reference measurements were obtained by suddenly pulling on the load arm to establish surface contact, it was noticed that the zero measurement changes with time over a period of several seconds. The direction of the change is consistent with the notion that the surfaces are warped during operation and become flat as the temperatures equalize following cut off of the steam flow. The total amplitude of the change has been from about 0.5 to 2 mils and varies inversely with the coolant temperature. Confirmation that the deformation of the bearing elements is such that the surfaces are convex is available from observations that contact and surface damage on collapse of the bearing has consistently occurred within the inner third of the bearing radius. The difficulty with this explanation is the fact that the measurements used for reference were obtained as soon as possible after contact of the surfaces, within a fraction of a second of contact. From this and the observed rate of change after the initial measurement, it seems unlikely that the entire difference between measured pressures and those expected from theoretical considerations is due to change in surface geometries during the time lag required to obtain a reference measurement. Nevertheless, in the absence of any other reasonable explanation, it is probable that error in the measurement of surface separation is principally responsible for the differences between measured and anticipated film pressures.

There is a discernable shift in the shape of the film pressure distribution with increasing load. If the characteristic sudden collapse

of the bearing is caused by interacting heat transfer and lubrication processes as was suggested earlier, the film pressure profile should respond to increasing load in the same general way as it responds to a reduction in coolant temperature. That is, an increase in load should cause the effective radius of the distributed pressure to move inward. This is the case especially for the experiments when coolant was circulated through the stator. The change in film pressure profile with successive increases in load is gradual and regular right up to the critical load which is the highest load for which data are given in Figures 10 through 12. In each case an increase in load of just 11.5 lbs was sufficient to bring the surface separation to zero and, to cause the film pressure to drop to zero except for small pressure at the innermost taps.

Film pressure distributions at the maximum load carried for different inlet steam pressures and constant coolant temperature are shown in Figure 12. There is relatively little difference in the shape of the pressure profile with changing inlet pressure. The increase in absolute values of film pressure, and in load carrying capacity, effected by raising inlet pressure from 60 to 80 psig is disproportionately large compared with the increase realized by raising inlet pressure from 40 to 60 psig. This feature of bearing performance was discussed previously, and as was mentioned then, may be associated with the fact that the surface separation corresponding to the critical load is also reduced as pressure is increased.

There was no consistent effect of rotational speed on film pressure distribution. Small differences were recorded but their direction was not consistent and they were small enough to be attributed to the fluctuation in inlet pressure caused by cycling of the pressure control on the steam generator (3 to 5 psig total range of fluctuation in pressure at the generator).

4.3 STATIONARY SURFACE TEMPERATURE

Measurements of stator surface temperature for the maximum load carried at different cooling rates are plotted in Figure 14. The thermodynamic equilibrium temperatures of the steam film based on the film pressure measurements are plotted also for comparison. Based on comparative shapes of the equilibrium steam and measured surface temperature profiles, the temperature and pressure measurements correlate nicely. The equilibrium steam temperatures are consistently higher than the measured surface temperatures and the difference is much greater at high cooling rates. Part of the difference may be explained by a small recession of the thermocouple junctions below the surface because of the sheath thickness. However, the sheath thickness is very small (probably about 3 to 5 mils) as compared to the thickness of the metal section between the top of the coolant passage and the surface. Therefore, the difference between surface and equilibrium steam temperatures is apparently caused mostly by a film of condensate on the cooled surface. The thermal conductivity of aluminum is about 300 times greater than that of water so a very thin film of water may represent a significant portion of the total conductive resistance from the steam layer to coolant. If there was no condensate film or its thickness was unchanged by a change in cooling rate, the ratio of the total temperature difference from steam layer to coolant to the temperature difference from the steam layer to the surface should be nearly constant. A comparison of these temperature ratios for the data given for 100 F and 170 F coolant in Figure 14 indicates that a greater proportion (by about 10 percent) of the total temperature drop occurred between the steam layer and the thermocouple junctions when the coolant temperature was 100 F. Evidently the condensate film was thicker for the lower coolant temperature. A very rough estimate of the condensate film thickness can be had from the following relationship:

$$\frac{T_{\text{steam}} - T_{\text{surface}}}{T_{\text{surface}} - T_{\text{coolant}}} = \frac{k_{\text{alum.}} \times t_{\text{water}}}{k_{\text{water}} \times t_{\text{alum.}}}$$

A typical distribution of temperatures is 250°F equilibrium steam temperature, 220 F surface and 100 F coolant temperature. The film thickness estimate for these temperatures is about 0.0002 inch.

Under most conditions, there was no appreciable change in the general shape of the temperature profile with increasing load up to and including the critical load. Higher loads resulted in a small general rise in temperatures approximately in proportion to the change in film pressures. Also in line with the change in film pressure profile, there usually was a slight tendency for the temperatures at the outermost measurement points to drop off more rapidly at the highest load. These conditions are illustrated by the temperature data for 60 psig steam and no coolant plotted in Figure 15. Occasionally when the shaft was stationary, there was a short-term stable point of operation with the bridging boundary at an intermediate radius. When this situation is obtained, the temperatures measured outside the bridging boundary drop off sharply apparently because the latent heat has already been removed from the film. The data for 60 psig steam, 140 F coolant temperature in Figure 15 illustrate this. The bridging boundary was located at a radius of about 1 3/4 inches during operation at 115 lb load during this experiment.

4.4 STEAM-COOLANT HEAT BALANCE

The heat withdrawn by the coolant from a unit mass of steam flowing through the bearing can be computed from the measured steam and coolant flow rates and the temperature rise in the coolant as it passes through the stator. The results of some of these computations for different coolant temperatures are plotted against load in Figure 16. There is a direct relationship between load and cooling rate which is to be expected from the combined effects of lower steam layer thickness and higher steam velocity. The more rapid increase in heat absorption by the coolant for a given load increment at low coolant temperatures may be explained by the lower bearing stiffness. The effects of rotation on heat transfer efficiency are shown by comparison of the results at 140 F coolant temperature with the disk stationary and rotating at 1000 rpm.

If all of the heat withdrawn from the steam were absorbed by the coolant and all of the steam were condensed inside the bearing (as indicated by the presence of a continuous bridging boundary) the heat gain by the coolant should balance the change in enthalpy from steam conditions at inlet to saturated water at atmospheric pressure. The bridging condition was met at 115 lb. load for the 140 F coolant, 0 rpm condition. However, the heat gain by the coolant is substantially lower than the equilibrium enthalpy loss from 60 psig steam to atmospheric water for this and all other operating conditions. Apparently there is a large rate of heat loss by conduction from the bearing area to other parts of the apparatus. No special effort was made to reduce conduction losses in the design of the apparatus so this is not too surprising. Some additional indication of the rate of heat loss by conduction can be had from the comparison of the measured film pressures when the coolant was drained from the stator and the theoretical pressure distribution for air as the lubricant (Figure 12).

4.5 EFFECT OF SUPERHEAT

One brief experiment was performed with steam superheated about 40°F over saturation temperature (60 psig. 345 F). This represents an increase in inlet steam enthalpy of about 20 Btu/lb and was the maximum amount of superheat which could be obtained since it was regularly necessary to supply a significant portion of the available superheater power to obtain dry steam at the bearing inlet. This amount of superheat resulted in no significant change in any of the bearing dependent variables except for an increase in the heat withdrawn by the coolant of about 10 Btu per pound of steam flow.

4.6 EROSION OF THE BEARING ELEMENTS

Erosion of the bearing elements, especially in the nozzle area has been considered as a potentially serious problem in vapor-lubricated bearings. This problem was given little consideration in the choice of bearing materials for these experiments since the principal objective was the study of lubrication processes. However, some very limited experience with erosion was gained and this will be described briefly as an indication of what might be expected.

Accumulated damage to the surfaces caused by brief periods of contact upon collapse of the bearing necessitated frequent changing of glass rotors and light refinishing of the stator surface so there was no opportunity to observe the effects of erosion after prolonged operation. However, there was one period of nearly 25 hours operation with the same surfaces which did result in some evidence of erosion. The glass rotor surface was lightly roughened or pitted in the nozzle area and there were a few short radial streaks extending from this area which were too lightly damaged for any roughness to be discernible by rubbing a finger nail across them. There was a significant amount of material removed from the stator surface in the nozzle and inner bearing areas - as much as about 2 or 3 mils outside the bell-mouthed inlet according to the amount of material which had to be removed from the surface outside this area to regain flatness. From the appearance of the surface during the subsequent refinishing operation it appeared that the effects of erosion were not uniform but that somewhat more material was removed in several scalloped areas extending over perhaps 45 degrees of arc.

It is believed that most of this erosion damage occurred during a brief period of operation when the surfaces were repeatedly separated considerably more than usual for short time intervals in an effort to induce hammering. This type of operation should cause high velocities and low steam quality which would be expected to greatly accelerate erosion. There was a noticeable increase in the film pressures measured at the innermost taps and an increase in load carrying capacity and steam flow rate immediately after this period of intermittent operation with large separations. These changes apparently resulted from the change in surface profile caused by erosion.

5.0 CONCLUSIONS

1. For all of the operating conditions investigated, there is a sharply defined load carrying limitation for the steam lubricated bearing beyond which there is a sudden loss of stiffness leading to collapse of the bearing and contact of the surface. The critical load coincides with the appearance near the outer bearing radius of a circumferential boundary in the film marking bridging of the surfaces by condensate. Collapse of the bearing is accompanied by a rapid inward movement of this boundary.
2. Bearing load carrying capacity and stiffness are strongly dependent on the rate at which heat is withdrawn from the film by the bearing surfaces. Increased cooling rate results in reduced stiffness and load capacity.
3. There is convincing evidence of the existence of a continuous condensate film on the cooled surface of the bearing for all conditions of operation when coolant was pumped through the stator. A rough estimate of condensate film thickness based on typical film surface and coolant temperatures is about 0.0002 inch.
4. Condensate in the form of droplets and streaks forms on the uncooled surface near the outer radius as the load approaches the critical load for collapse of the bearing. Bridging of the gap by condensate occurs first at these droplets and subsequently spreads to form a complete boundary.
5. Comparison of the performance of the experimental bearing lubricated with steam with its theoretical performance using a single-phase lubricant having the properties of dry steam indicates that for a fixed inlet pressure and surface separation, a two-phase bearing has considerably lower load carrying capacity. A reduced load carrying capacity can be

explained by progressive mass transfer from the vapor to the liquid state as the steam flows over the cooled surface. Same phenomenon explains the inverse relationship between cooling rate and load carrying capacity.

6. For the bearing configuration used here (stationary cooled surface) there was very little dependence of bearing performance on rotor speed.

7. Instability or "hammering", in which the gap between surfaces of the bearing fluctuates cyclically has been observed occasionally when the shaft is stationary and conditions at onset were such that the bearing was close to the verge of collapse. The vibration is usually damped out within a few seconds.

RECOMMENDATIONS

1. An experimental study of the steam-lubricated bearing with inverted elements; adiabatic stationary surface above a cooled rotating surface, should be performed. The effects of rotation on the condensation process and its consequences such as reduction of load capacity, hammering, and bearing collapse as reported here will be of particular interest.

2. The design of future experimental apparatus more attention should be given to minimizing thermal distortion of the bearing surfaces even though accomplishing this may reduce the rate of cooling which can be achieved.

LIST OF REFERENCES

1. I. Beretsky, "Two-Phase Flow in Thrust Bearings.
Part I - Derivation of Equations", MTI-62TR9,
prepared for ONR under Contract No. Nonr-3731(00)
(FBM), June, 1962.
2. L. Licht and D. D. Fuller, "A Preliminary Investi-
gation of an Air Lubricated Hydrostatic Thrust
Bearing", ASME Paper No. 54 Lub. 18, Oct, 1954.

FIGURES

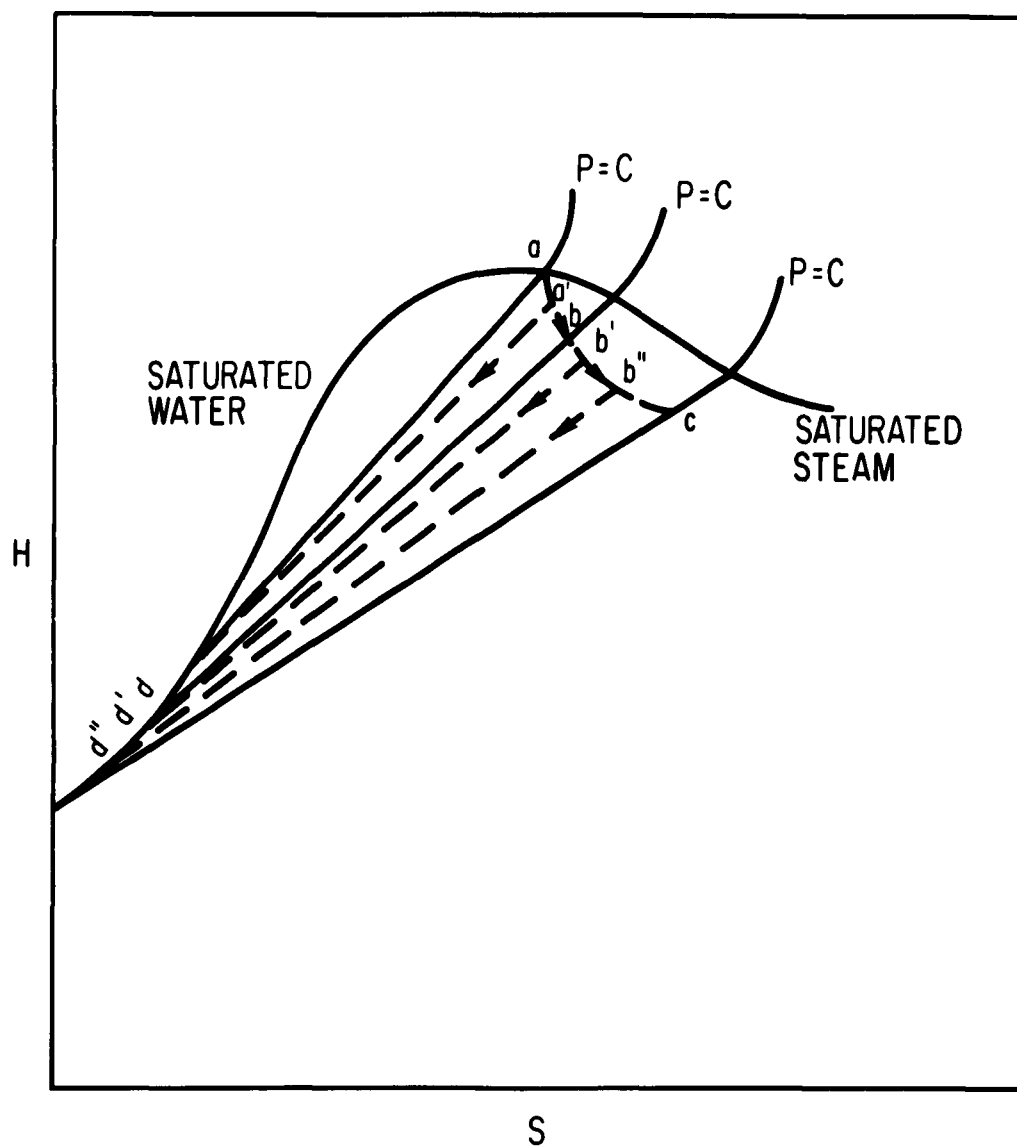


FIG. 1 MOLLIER CHART REPRESENTATION OF BEARING STEAM FLOW PROCESS

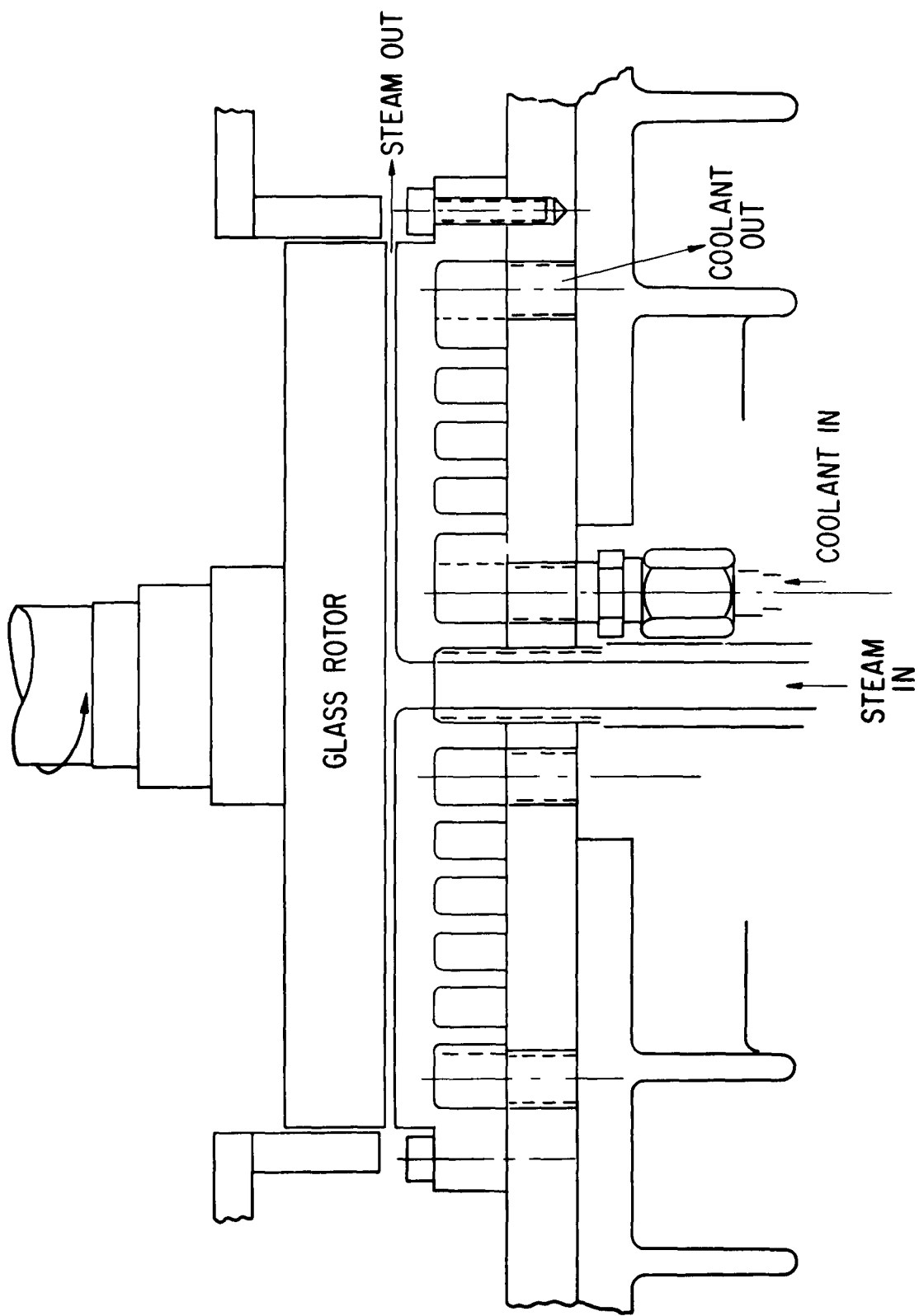


FIG. 2 CROSS SECTIONAL VIEW OF EXPERIMENTAL BEARING

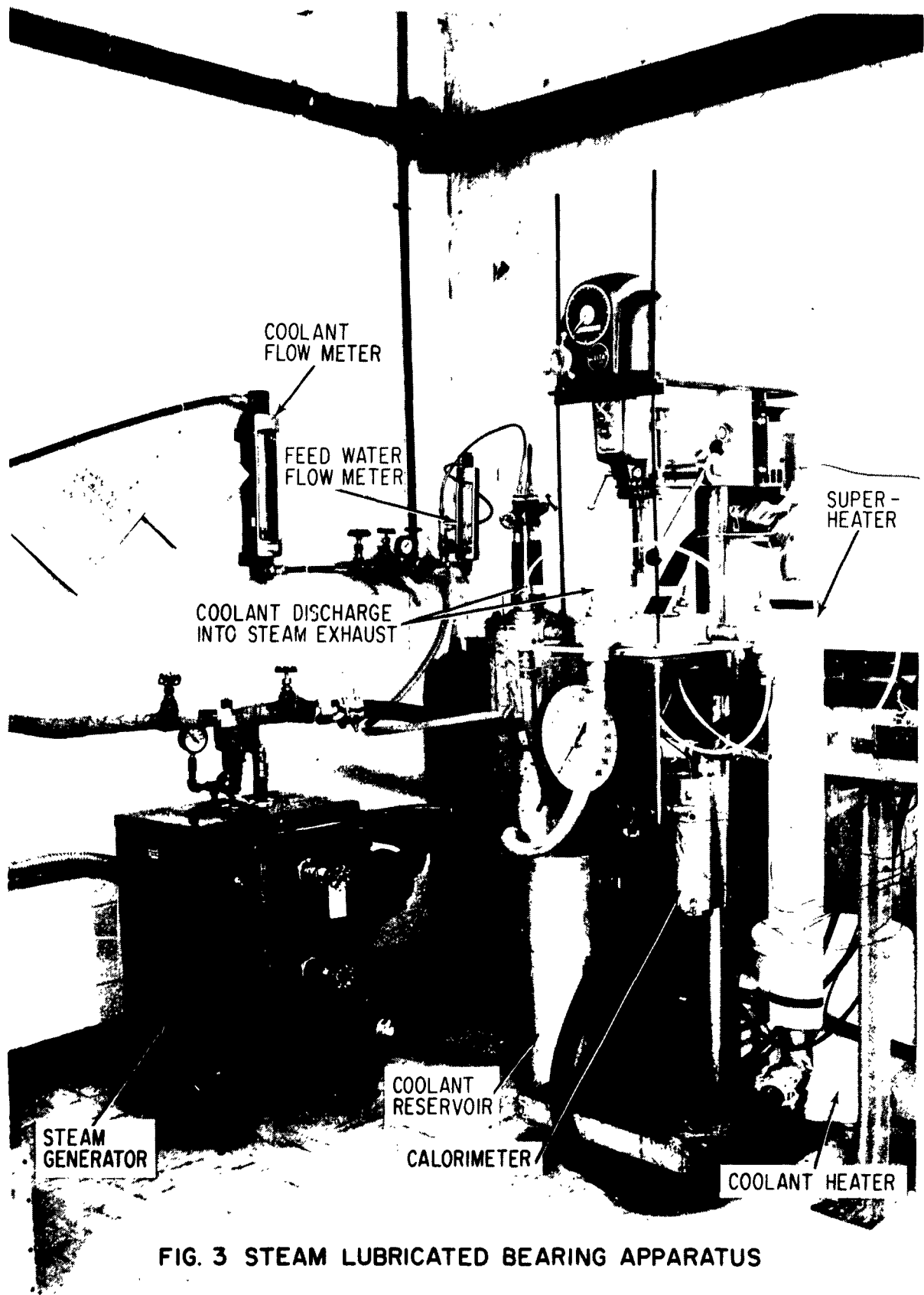


FIG. 3 STEAM LUBRICATED BEARING APPARATUS

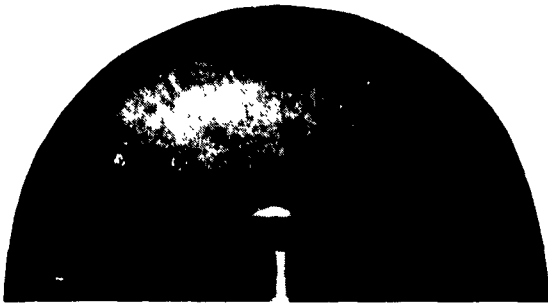


Fig. 4 View of Bearing Interface Showing Condensate Droplets.

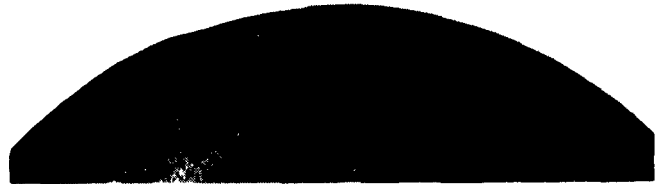


Fig. 5 View of Bearing Interface Showing Partial Condensation.

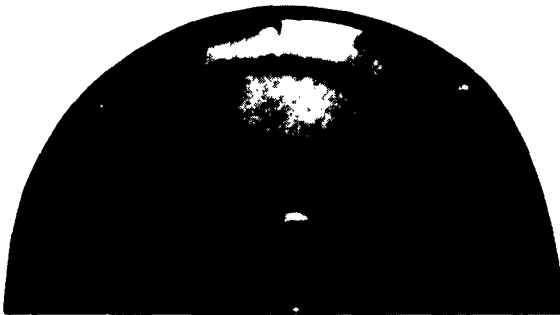


Fig. 6 View of Bearing Interface Showing Bridging Boundary Near Outer Edge.



Fig. 7 View of Bearing Interface Showing Bridging Boundary Near the Inlet.

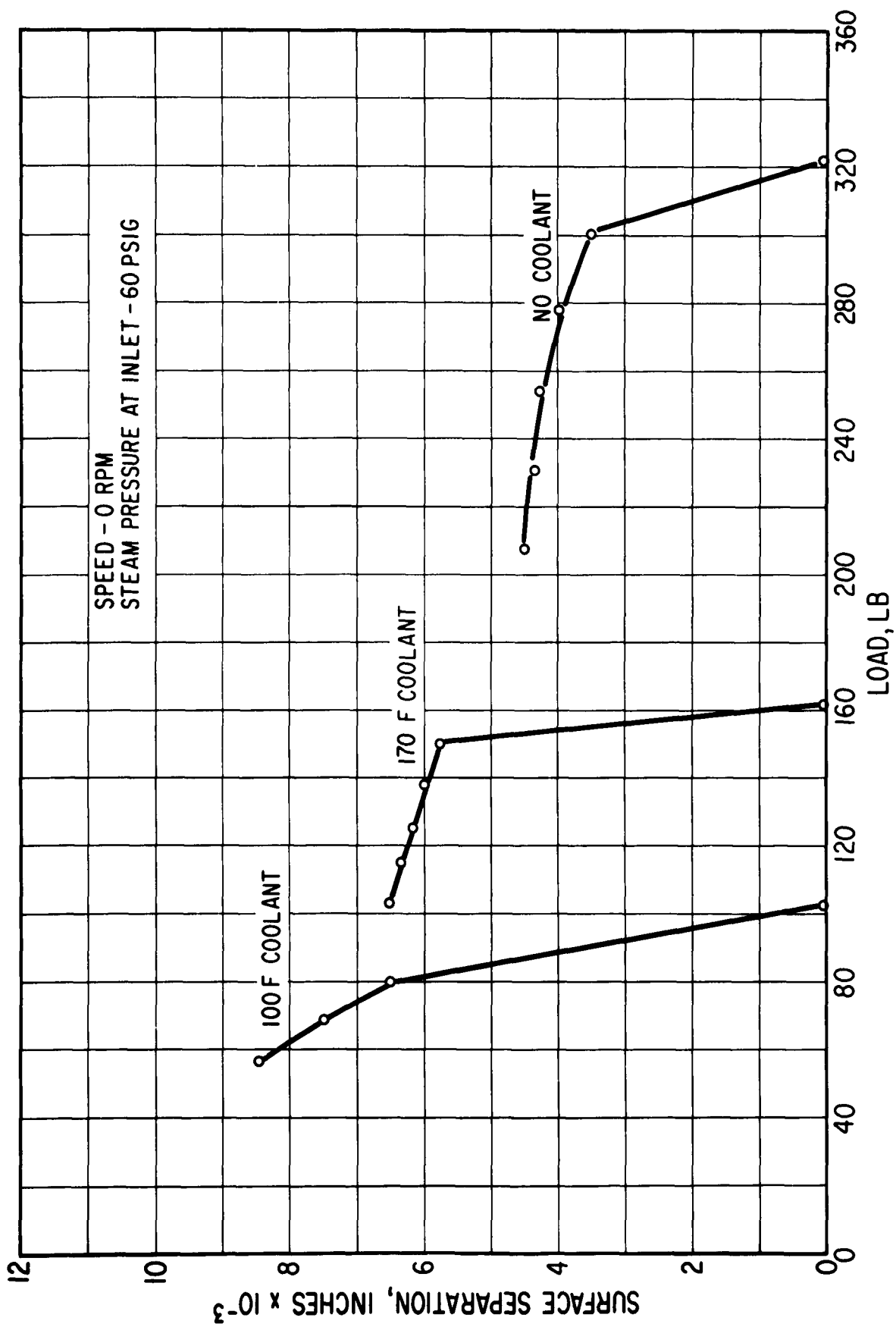


FIG. 8 EFFECT OF COOLING RATE ON BEARING STIFFNESS

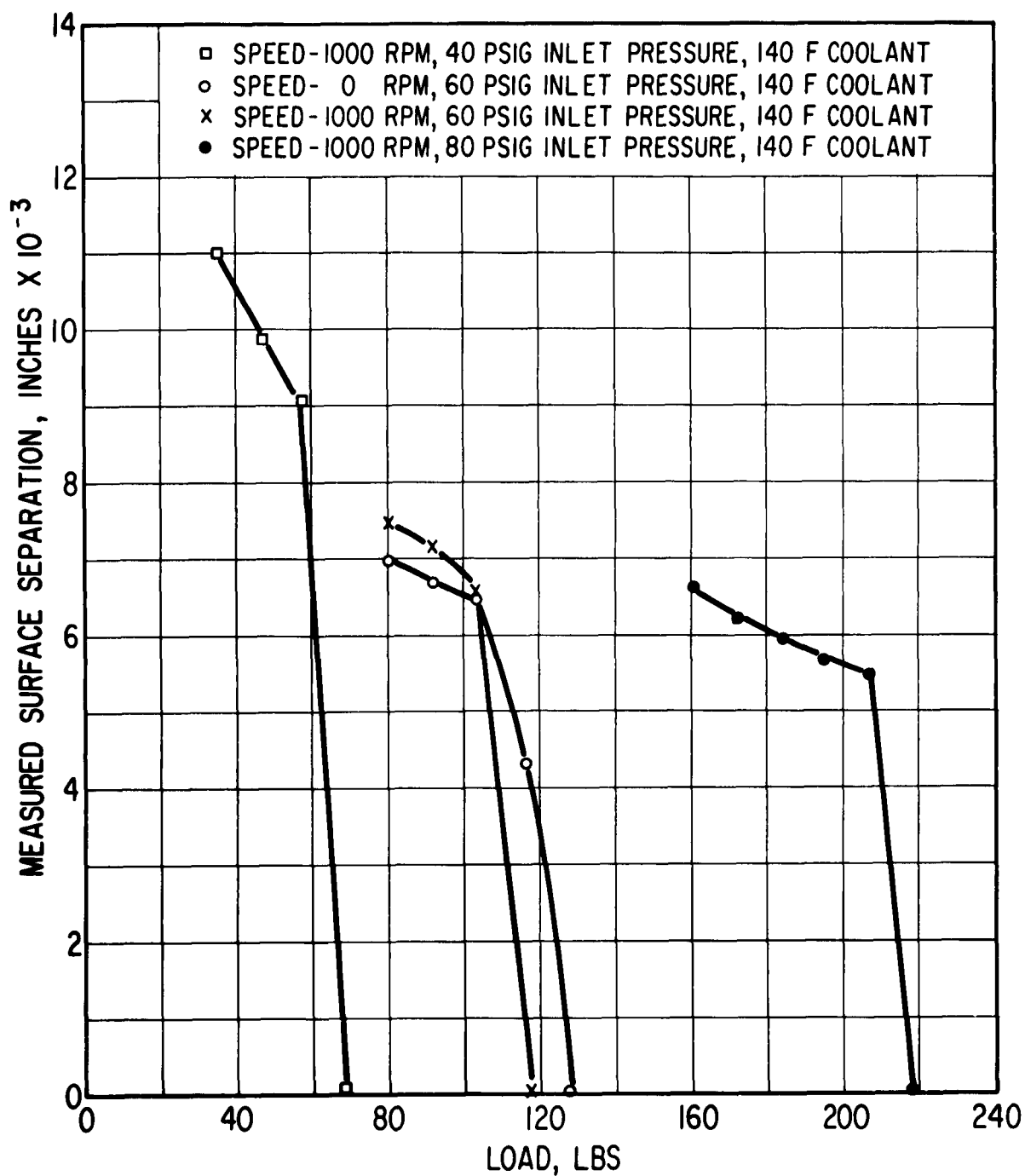


FIG. 9 EFFECT OF INLET PRESSURE ON BEARING STIFFNESS

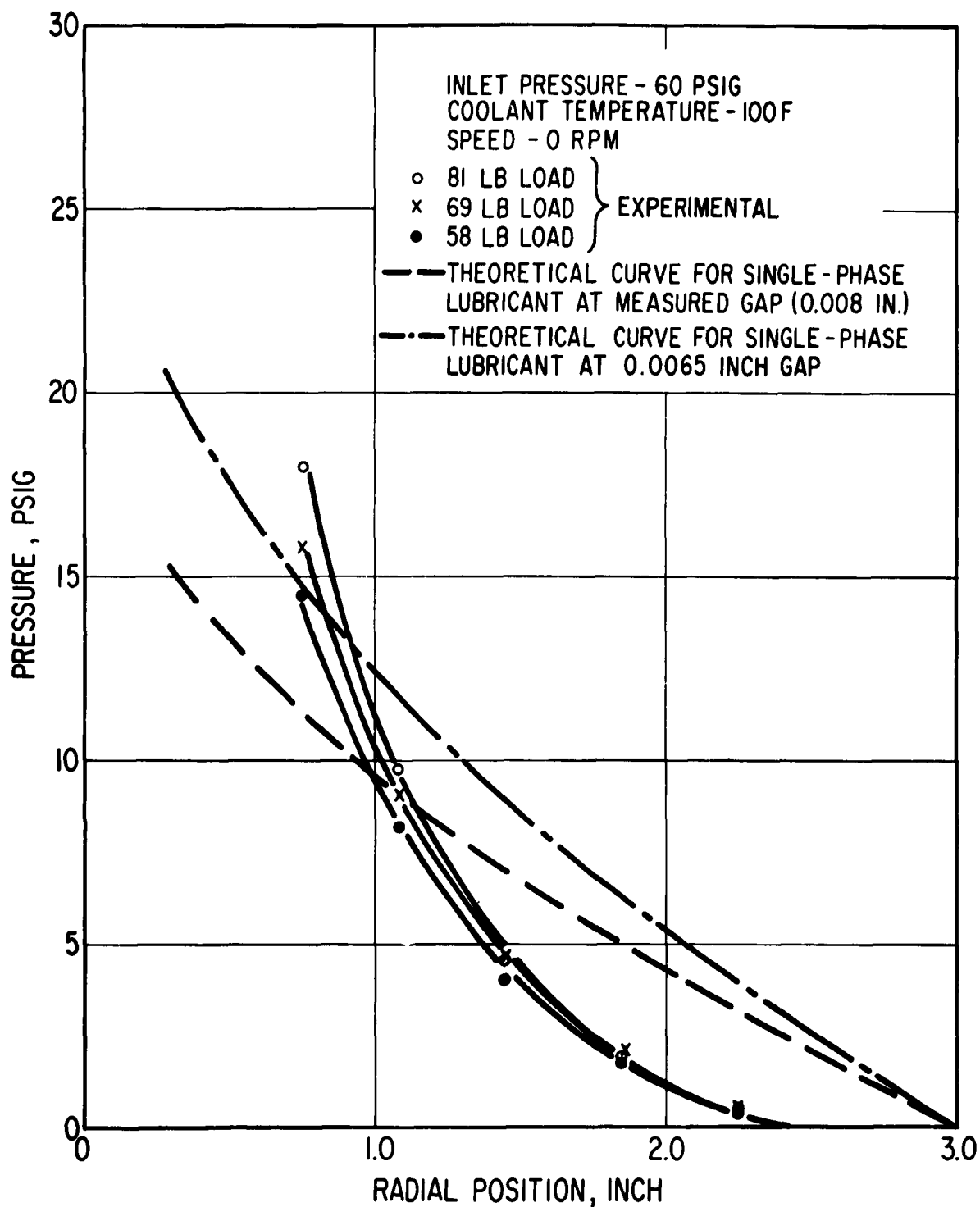


FIG. 10 FILM PRESSURE DISTRIBUTION WITH 100 F COOLANT

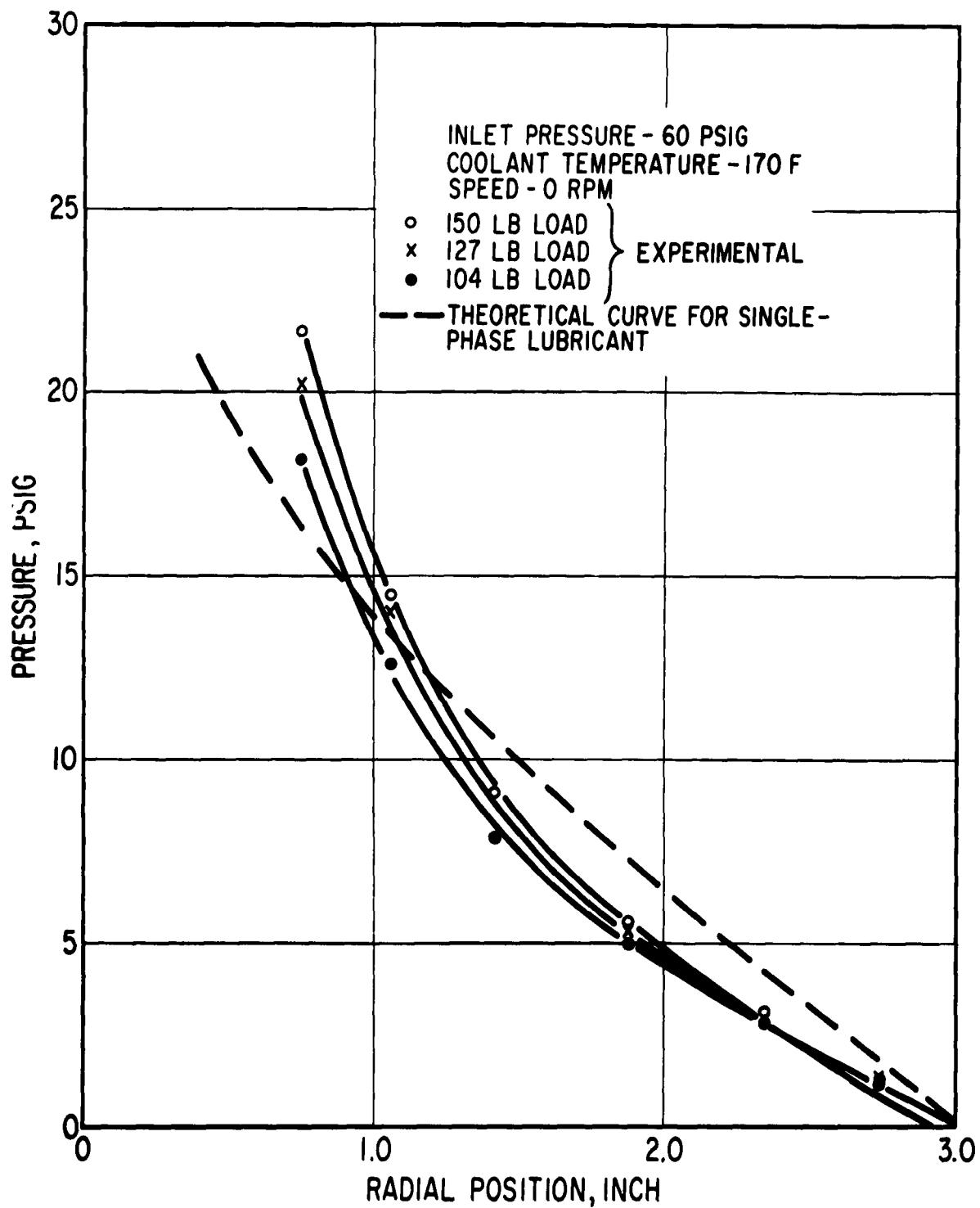


FIG. II FILM PRESSURE DISTRIBUTION FOR 170 F COOLANT

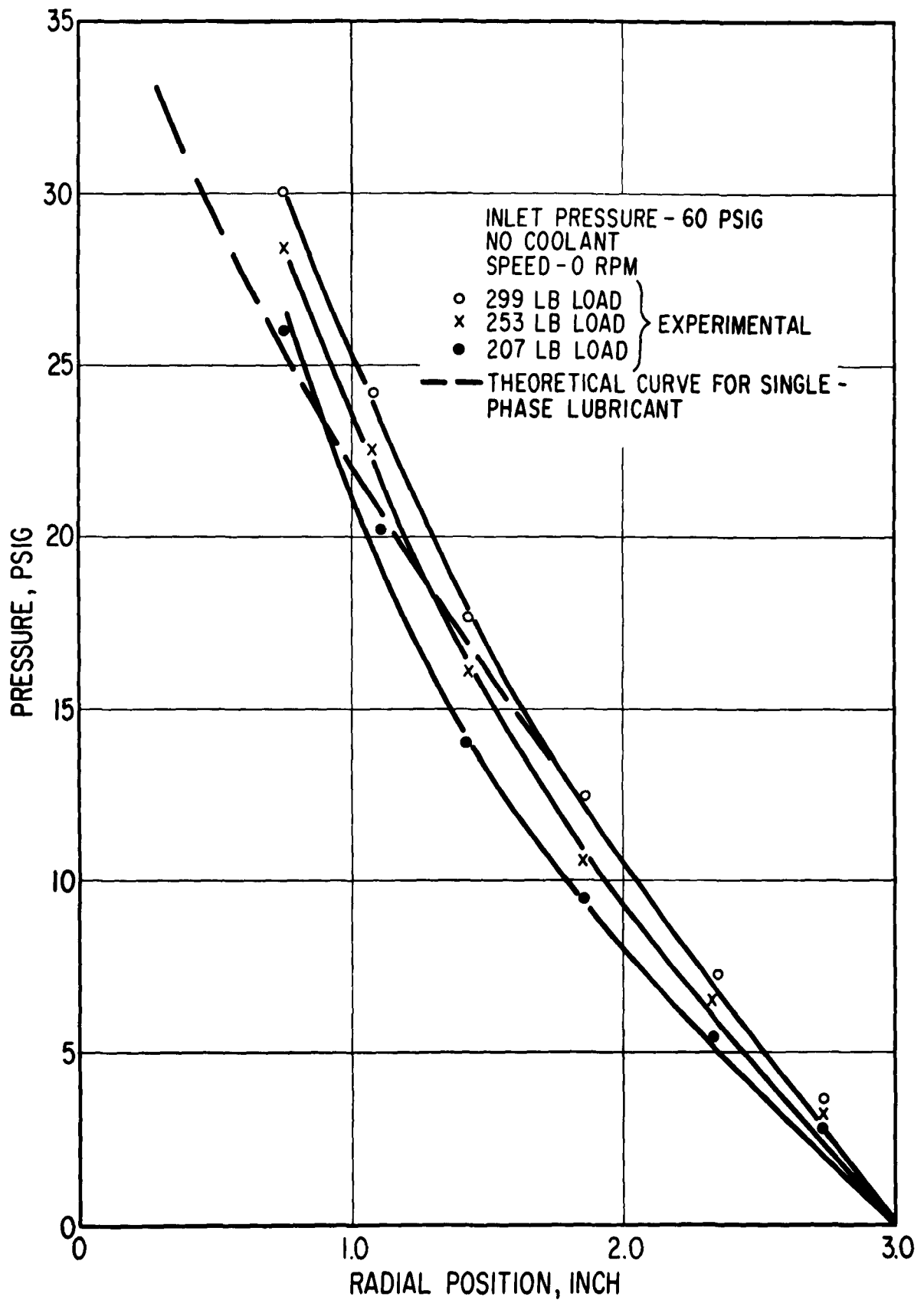


FIG. 12 FILM PRESSURE DISTRIBUTION WITH NO COOLANT

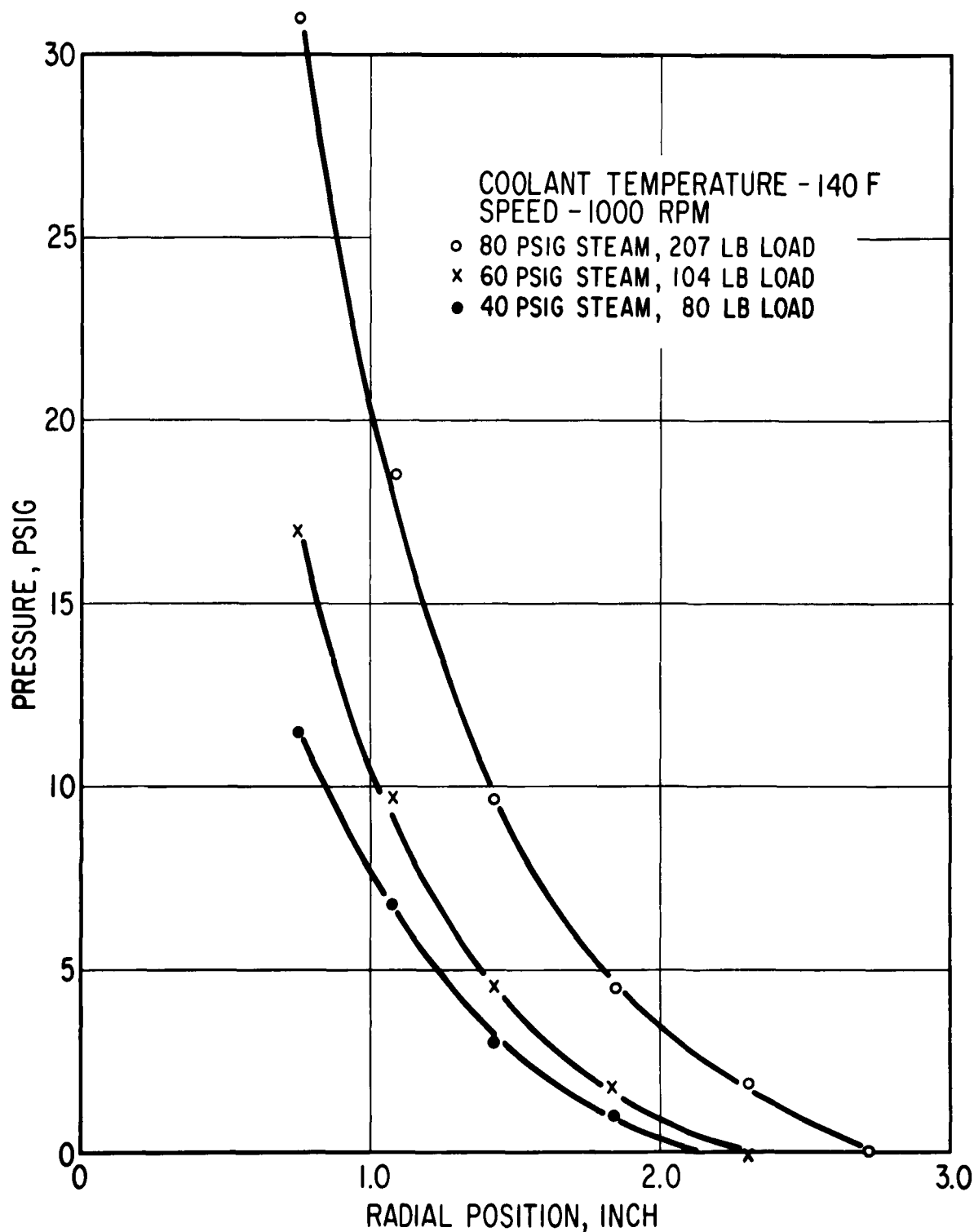


FIG. 13 FILM PRESSURE DISTRIBUTION FOR DIFFERENT INLET PRESSURES

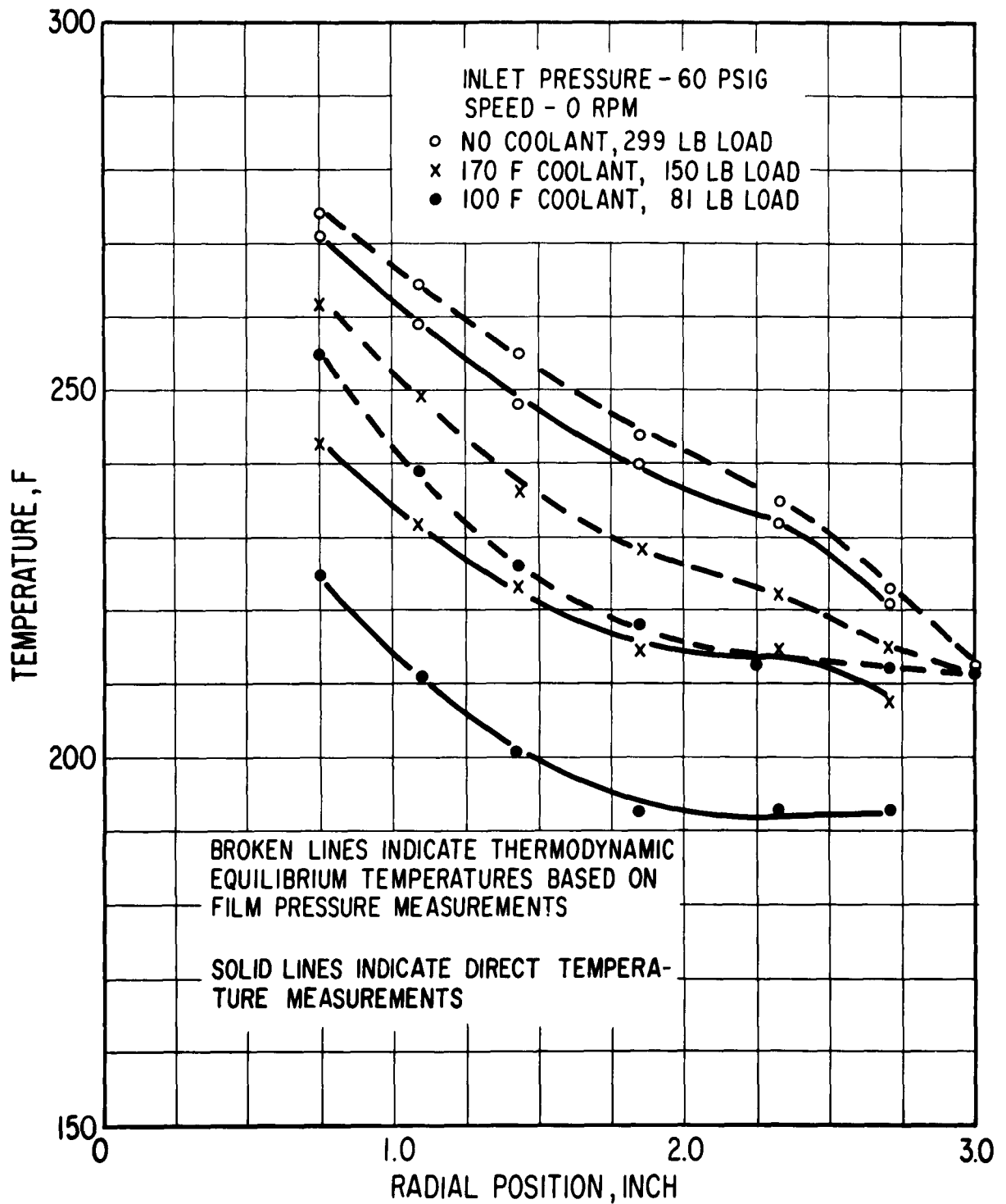


FIG. 14 STATIONARY SURFACE TEMPERATURES AT DIFFERENT COOLING RATES

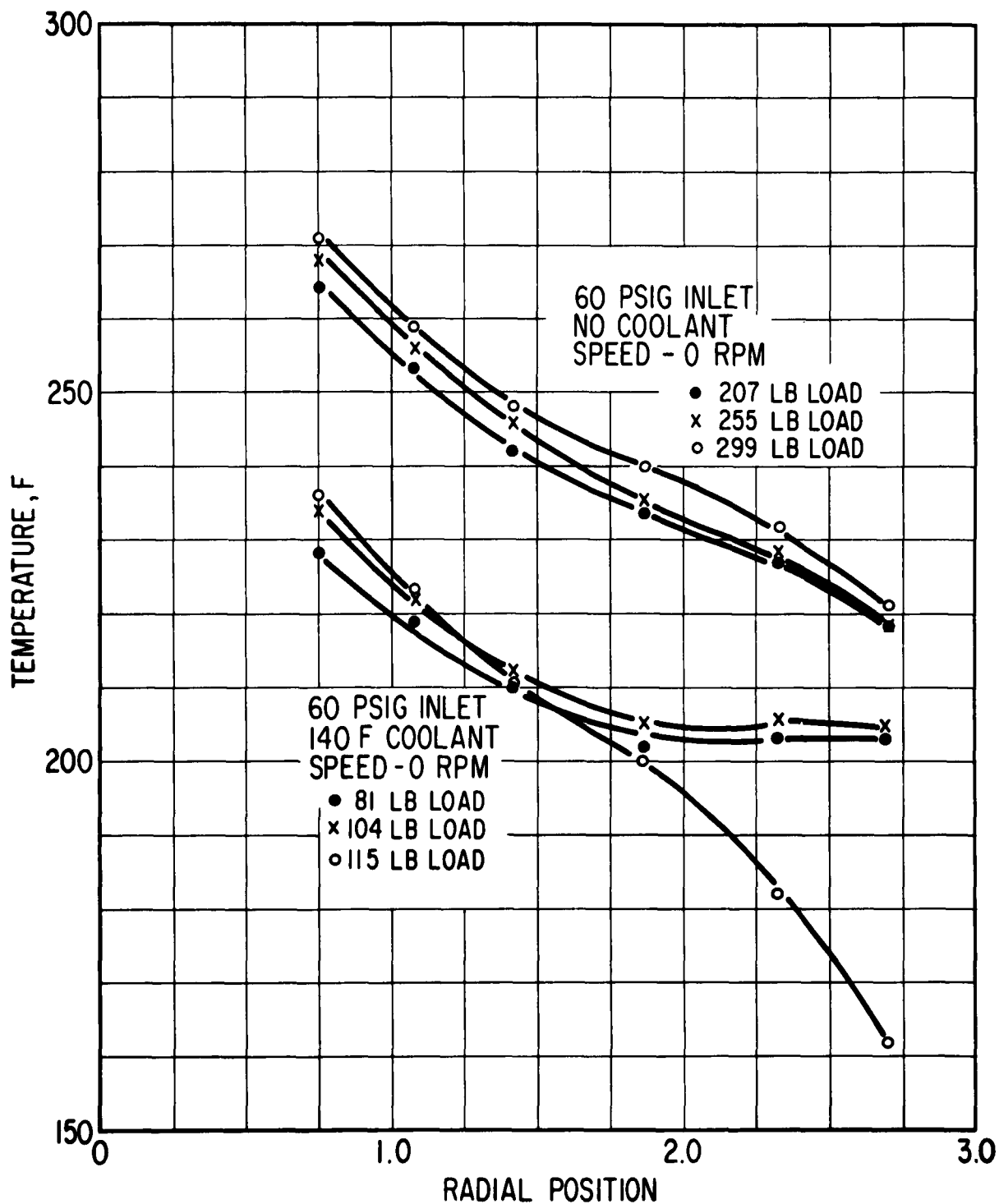


FIG. 15 EFFECT OF LOAD ON STATOR SURFACE TEMPERATURES

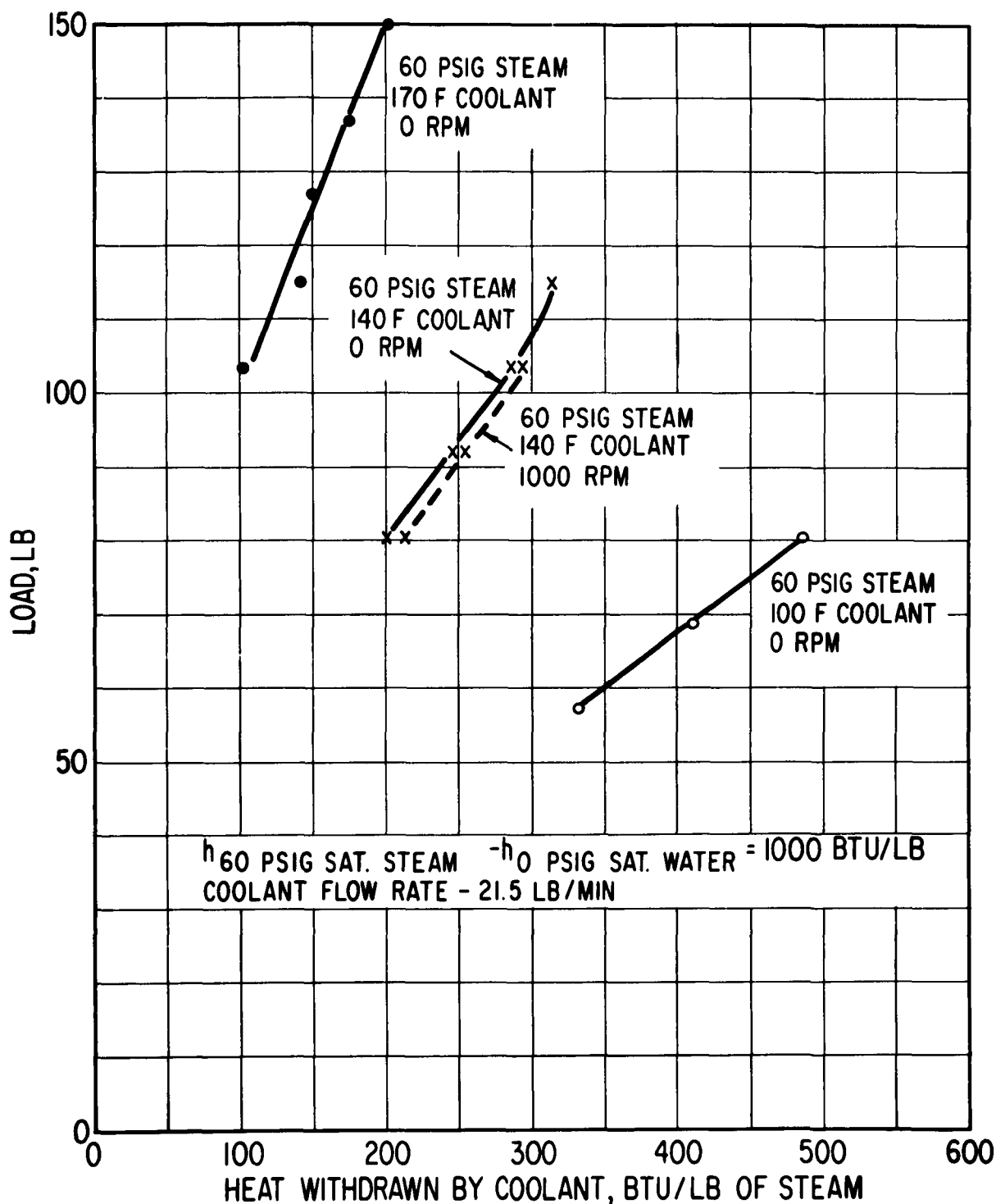


FIG. 16 HEAT BALANCE FOR SEVERAL COOLANT TEMPERATURES

APPROVED DISTRIBUTION LISTS FOR UNCLASSIFIED TECHNICAL REPORTS
ISSUED UNDER
PROCESS FLUID LUBRICATION CONTRACTS

| | | | |
|---|--|---|---|
| Chief of Naval Research Department of the Navy Washington 25, D. C. Attn: Code 438 | Director Naval Research Laboratory Washington 25, D. C. Attn: Code 2000 | 3 | 1 |
| 429 | 5230 | 1 | 1 |
| 466 | Special Projects Office Department of the Navy Washington 25, D. C. Attn: Code SP23-A (D. Gold) | 1 | 1 |
| Commanding Officer Office of Naval Research Branch Office Tenth Floor The John Crerar Library Bldg. 86 East Randolph Street Chicago, Illinois | Head, Bearings and Seals Branch U. S. Naval Engineering Experiment Station Annapolis, Maryland Attn: Code 851 (Watt V. Smith) | 1 | 1 |
| Commanding Officer Office of Naval Research Branch Office 346 Broadway New York 13, New York | Material Laboratory Library Building 291, Code 912B New York Naval Shipyard Brooklyn 1, New York | 1 | 1 |
| Commanding Officer Office of Naval Research Branch Office Box 39, Navy #100 Fleet Post Office New York, New York | Library Technical Reports Section U. S. Naval Postgraduate School Monterey, California | 1 | 1 |
| Commanding Officer Office of Naval Research Branch Office 1030 East Green Street Pasadena 1, California | Commanding Officer U. S. Naval Avionics Facility Indianapolis 18, Indiana Attn: J. G. Weir | 1 | 1 |
| Commanding Officer Office of Naval Research Branch Office 1000 Geary Street San Francisco 9, California | Director U. S. Naval Boiler and Turbine Lab. Naval Base Philadelphia 12, Pennsylvania | 1 | 1 |
| Chief, Bureau of Ships Department of the Navy Washington 25, D. C. Attn: Code 644B (James C. Reid, Jr.) | Office of Chief of Ordnance Research and Development Division Department of the Army Washington 25, D. C. Attn: Norman L. Klein | 1 | 1 |
| Chief, Bureau of Naval Weapons Department of the Navy Washington 25, D. C. Attn: Code RAAR-3431 (G. D. Norman) | Fuels & Lubricants Section Research Branch Research & Development Division Office, Chief of Ordnance Attn: Mr. Ronald E. Stroets 4th Floor, Pentagon Annex #2 Washington 25, D. C. | 1 | 1 |

Page 2

| | | | |
|---|--|----|---|
| Chief of Research and Development Office, Chief of Staff Department of the Army Pentagon Building Washington 25, D. C. | Office of Assistant Director (Army Reactors) Division of Reactor Development U. S. Atomic Energy Commission Washington 25, D. C. Attn: Mr. Clarence E. Miller, Jr. | 1 | 2 |
| Commanding General U. S. Army Engineer R&D Laboratories Fort Belvoir, Virginia Attn: W. H. Crim, Nuclear Power Field Office | Chief Engineering Development Branch Reactor Development Division U. S. Atomic Energy Commission Washington 25, D. C. | 2 | 1 |
| Director U. S. Army Engineer Research and Development Laboratory Fort Belvoir, Virginia Attn: Technical Documents Center | Headquarters Library U. S. Atomic Energy Commission Washington, D. C. | 1 | 1 |
| Commander Army Rocket & Guided Missile Agency Redstone Arsenal, Alabama Attn: Technical Library | Chief, Division of Engineering Maritime Administration GAO Building Washington 25, D. C. | 1 | 1 |
| ESD - AROD Box CM, Duke Station Durham, North Carolina | Cryogenic Engineering Laboratory National Bureau of Standards Boulder, Colorado Attn: Library | 1 | 1 |
| Chief of Staff, U. S. Air Force The Pentagon Washington 25, D. C. Attn: AFDR-AS/M | Mr. Harold Hensing National Aeronautics and Space Administration 1512 H. Street, N. W. Washington 25, D. C. | 1 | 1 |
| Commander Air Force Office of Scientific Research Washington 25, D. C. Attn: SRHM | Mr. Edmund E. Bisson Chief, Lubrication & Wear Branch Lewis Research Center National Aeronautics and Space Administration 21000 Brookpark Road Cleveland, Ohio | 1 | 1 |
| Commander Aeronautical Systems Division of the Air Force Systems Command Wright-Patterson AF Base, Ohio Attn: ASRML-2, J. L. Morris | Mr. Rudolph E. Beyer George C. Marshall Space Flight Center National Aeronautics and Space Administration Guidance and Control Division Gyro-Stabilizer Branch Huntsville, Alabama | 2 | 3 |
| ASRMD, P. C. Hanlon | | 1 | |
| ASRMP-1, B. L. McFadden, Jr. | | 1 | |
| ASRMOO-1, R. W. McAdony | | 1 | |
| Armed Services Technical Information Agency Arlington Hall Station Arlington 12, Virginia | Mr. H. W. Savage Oak Ridge National Laboratory Post Office Box Y Oak Ridge, Tennessee | 10 | 1 |

Page 3

| | | | |
|---|--|---|---|
| Chief, Technical Information Service Extension P. O. Box 62 Oak Ridge, Tennessee Attn: Melvin S. Day | Massachusetts Institute of Technology Instrumentation Laboratory 68 Albany Street Cambridge 39, Massachusetts Attn: Library, W1-109 | 1 | 1 |
| Applied Physics Laboratory Johns Hopkins University Silver Spring, Maryland Attn: George L. Seidelstad, Supr., Tech., Reports Group | Franklin Institute Laboratory for Research and Development Philadelphia, Pennsylvania Attn: Professor D. D. Fuller | 1 | 3 |
| Department of Chemical Engineering New York University New York 53, New York Attn: James J. Barker, Assoc. Prof. of Nuclear Engineering | Library Institute of Aerospace Sciences 2 East 64th Street New York, New York | 1 | 1 |
| Resident Representative Office of Naval Research c/o University of Pennsylvania 3438 Walnut Street Philadelphia 4, Pennsylvania | Mr. G. B. Spoon Sr. Member, Technical Staff ITT Federal Laboratories Division of International Telephone and Telegraph Corporation 15151 Bledsoe Street San Fernando, California | 1 | 1 |
| Professor P. R. Trumpler Towne School of Civil and Mechanical Engineering University of Pennsylvania Philadelphia, Pennsylvania | Aerospace Corporation P. O. Box 95085 Los Angeles 45, California Attn: Aerospace Library Technical Reports Group | 1 | 1 |
| Jet Propulsion Laboratory California Institute of Technology 4800 Oak Grove Avenue Pasadena, California Attn: Library | AirResearch Manufacturing Company Sky Harbor Airport 402 South 36th Street Phoenix, Arizona Attn: Mr. VanDerwagen Librarian | 1 | 1 |
| Illinois Institute of Technology Chicago 16, Illinois Attn: Professor L. N. Tao | American Society of Lubrication Engineers 5 North Wabash Avenue Chicago 2, Illinois | 1 | 1 |
| Professor M. C. Shaw, Head Department of Mechanical Engineering Carnegie Institute of Technology Pittsburgh 13, Pennsylvania | Chairman Research Committee on Lubrication The American Society of Mechanical Engineers United Engineering Center 345 East 47th Street New York 17, New York | 1 | 1 |

Page 4

| | | | |
|--|--|---|---|
| Mr. C. R. Adams Physics Technology Department Aero-Space Division The Boeing Company Seattle 24, Washington | Mr. L. W. Winn General Electric Company Aircraft Accessory Turbine Department 950 Western Avenue, Bldg. 3-74 Lynn, Massachusetts | 1 | 1 |
| Mr. B. W. Birmingham Cryogenic Engineering Laboratory National Bureau of Standards Boulder, Colorado | Hydraulics, Incorporated 200 Monroe Street Rockville, Maryland | 1 | 1 |
| Ford Instrument Company 31-10 Thomson Avenue Long Island City 1, New York Attn: Mr. Jarvis | International Business Machine Corp. Research Laboratory San Jose, California Attn: Dr. W. E. Langlois | 1 | 2 |
| Mr. Adolf Egli Ford Motor Company Engineering and Research Staff P. O. Box 2053 Dearborn, Michigan | Dr. J. S. Ausman Littion Systems, Inc. 5500 Canoga Avenue Woodland Hills, California | 1 | 1 |
| Dr. John E. Mayer, Jr. Non-Metallics Section Applied Science Department Scientific Laboratory Ford Motor Company P. O. Box 2053 Dearborn, Michigan | Mr. Don Moors Littion Systems 5500 Canoga Avenue Woodland Hills, California | 1 | 1 |
| AirResearch Manufacturing Division The Garrett Corporation 9851 S. Sepulveda Boulevard Los Angeles, California Attn: Jerry Glaser, Supervisor Mechanical Lab.-Dept. 93-17 | Dr. Beno Sternlicht Mechanical Technology Incorporated 1 Herbert Drive Latham, New York | 1 | 3 |
| General Atomics Division General Dynamics Corporation P. O. Box 608 San Diego 12, California Attn: Mr. F. W. Simpson | Mr. J. W. Lower Chief, Engineer-Inertial Components Honeywell Aero Division 2600 Ridgway Road Minneapolis, Minnesota | 1 | 1 |
| Bearing and Lubricant Center General Engineering Laboratory General Electric Company 1 River Road Schenectady, New York Attn: G. R. Fox, Manager | Mrs. Alice Ward, Librarian Norden Division of United Aircraft Corp. Helen Street Norwalk, Connecticut | 1 | 1 |
| | Autonetics Division (Librarian) North American Aviation Inc. 9150 East Imperial Highway Downey, California | 1 | 1 |
| | Northrop Corporation Repair Division 1001 East Broadway Burbank, California Attn: Technical Information, 3125 | 1 | 1 |